2006

Ferromagnetic Resonance Investigations on Ga0.965Mn0.035As Film

S. Balascuta

X. Liu

D. V. Baxter

J. Carini

T. Wojtowicz

See next page for additional authors

Recommended Citation

Balascuta, S., et al. "Ferromagnetic Resonance Investigations on Ga0.965Mn0.035As Film." Journal of Applied Physics, vol. 99, no. 11, American Institute of Physics, June 2006, p. 113908, doi:10.1063/1.2193062.

Ferromagnetic resonance investigations on $Ga_{0.965}Mn_{0.035}As$ film

S. Balascuta
Department of Physics, Indiana University, Bloomington, Indiana 47401

X. Liu and D. V. Baxter
Department of Physics, University of Notre Dame, Notre Dame, Indiana 46556

J. Carini
Department of Physics, Indiana University, Bloomington, Indiana 47401

T. Wojtowicz
Department of Physics, University of Notre Dame, Notre Dame, Indiana 46556 and Institute of Physics, Polish Academy of Sciences, Warszawa, Poland

Y. Sasaki and J. Furdyna
Department of Physics, University of Notre Dame, Notre Dame, Indiana 46556

M. Chipara[a)]
Department of Chemistry, Indiana University, Bloomington, Indiana 47405

(Received 3 October 2005; accepted 8 March 2006; published online 15 June 2006)

Ferromagnetic resonance studies of the temperature dependence of magnetic anisotropies in a $Ga_{0.965}Mn_{0.035}As$ film between 5 and 40 K are reported. The in-plane and out-of-the-plane angular dependences of the resonance field were analyzed within the Landau-Lifshitz-Gilbert approach. The second- and fourth-order magnetic anisotropy energies were derived. The temperature dependence of magnetization and of magnetic anisotropy were studied by superconducting quantum interference device and ferromagnetic resonance. © *2006 American Institute of Physics*.
[DOI: 10.1063/1.2193062]

I. INTRODUCTION

Ferromagnetic resonance (FMR) is a powerful tool for investigating magnetic anisotropies in thin films,[1] interlayers,[2,3] and diluted magnetic semiconductors such as $Ga_{1-x}Mn_xAs$.[4] FMR studies of the first- and second-order magnetic anisotropies were reported on $Ga_{1-x}Mn_xAs$,[5] $Ga_{1-x}Mn_xAs$ with MnAs clusters,[6] and InGaMnAs.[7] These materials are possible candidates in the production of spin-dependent magneto-optical and magnetoelectrical devices. It has been shown that $Ga_{1-x}Mn_xAs$ films show a strong magnetic anisotropy.[5,8] Under the compressive or tensile strain, the easy axis of $Ga_{1-x}Mn_xAs$ films is either parallel or perpendicular to the film plane, respectively.[7,8] The angular dependence of the resonance field, H_0, was used to determine the g factor, the magnetic anisotropy constants, and the interlayer magnetic coupling for films and multilayers.[9] In this paper, detailed measurements and analysis of resonance line position are reported. In the present study FMR is used to investigate the temperature dependence of magnetic anisotropy constants for a $Ga_{1-x}Mn_xAs$ ($x=0.035$) film with 300 nm thickness.

II. EXPERIMENTAL METHODS

A nonequilibrium low-temperature molecular beam epitaxy (MBE) method was used to grow the $Ga_{1-x}Mn_xAs$ film with $x=3.5\%$ Mn on a GaAs(100) Si substrate.[10] During the growth, the surface quality of the sample was monitored *in situ* by reflection high-energy electron diffraction (RHEED).[11] A 0.4 mm thick GaAs substrate was first deoxidized at 600 °C, and then a 100 nm GaAs buffer layer was grown to obtain the atomic flat surface. After that the temperature of the substrate was decreased to 275 °C. Finally, a 100 nm thick low-temperature GaAs buffer layer and a 300 nm thick $Ga_{1-x}Mn_xAs$ ($x=3.5\%$) magnetic layer were grown. The Mn concentration was determined by x-ray diffraction measurements of the vertical lattice constant of the tetragonally distorted $Ga_{1-x}Mn_xAs$ film. The FMR absorption curves were measured in the X band (microwave frequency about 9.4 GHz), using a Bruker ESP 300 electron paramagnetic resonance (EPR) spectrometer, equipped with a variable temperature accessory.

The obtained film had a crystalline tetragonal symmetry with Mn ions distributed randomly in the GaAs lattice.[12] The samples were cleft along the [110] and $[1\bar{1}0]$ crystalline directions. The angular dependence of FMR spectra was recorded in the configurations shown in Fig. 1. The polar and azimuthal angles of the magnetization **M** and magnetic field **H** are (θ,φ) and (θ_H,φ_H) respectively. The dependence of the resonance signal on the orientation of the film relative to the static magnetic field was studied. The [001] crystalline direction is normal to the plane of the film and the ox and oy axes are parallel with the [100] and [010] crystalline directions, respectively; θ_H and φ_H are the angles between the direction of the magnetic field **H** and the oz and ox axes, respectively. Therefore, in configuration A the magnetic field

[a)]Author to whom correspondence should be addressed; FAX: (812) 855 8000; electronic mail: mchipara@indiana.edu

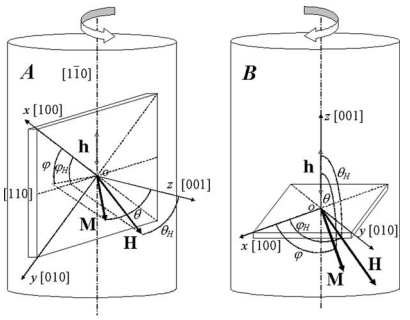

FIG. 1. The coordinate systems used for the measurements and analysis of the angular dependence. (A) The EPR tube is rotated about the $[1\bar{1}0]$ axis. The magnetic field "rotates" in the $(1\bar{1}0)$ plane normal to the surface of the film. The [001] direction is perpendicular to the film and to the wall of the quartz tube. (B) The EPR tube is rotated about the oz axis. The magnetic field is confined in the plane of the film. The [001] crystalline direction is parallel to the wall of the quartz tube.

rotates within the $(1\bar{1}0)$ plane, while in configuration *B* the magnetic field rotates within the (001) plane. In addition to FMR measurements, temperature dependence of the magnetization in two magnetic fields (0.005 and 0.3 T) and field dependence of the magnetization at constant temperature were measured by using a superconducting quantum interference (SQUID) magnetometer.

III. THEORETICAL MODEL

The free energy density of a film with tetragonal symmetry (such as $Ga_{1-x}Mn_xAs/GaAs$) is[13,14]

$$F = -\mu_0 \mathbf{H}\cdot\mathbf{M} + \frac{\mu_0 D M^2}{2}\alpha_z^2 - K_n\alpha_z^2 - \frac{K_{4\perp}}{2}\alpha_z^4 - \frac{K_{4\parallel}}{2}(\alpha_x^4+\alpha_y^4) - K_U\frac{(\hat{n}_1\mathbf{M})^2}{M_S^2}. \quad (1)$$

The first and second terms represent the Zeeman and the demagnetization energy (*D* is the demagnetization factor). The third and fourth terms (K_n and $K_{4\perp}$) are the second-order and fourth-order anisotropies perpendicular to the film plane. The fifth term ($K_{4\parallel}$) is the fourth-order in-plane magnetic anisotropy. The sixth term (K_u) is the in-plane uniaxial magnetic anisotropy along the in-plane direction defined by the unit vector $\mathbf{n}_1$ parallel with the [110] crystalline direction. From the physical point of view, the in-plane uniaxial magnetic anisotropy term expresses the deviation of the local symmetry from the theoretical fourfold symmetry. This term is extremely important and under intense debate as it expresses the deviation of the magnetic properties of the actual sample from the theoretical intrinsic magnetic properties. The magnetic anisotropy fields corresponding to the term included in the free energy expression (1) are $H_{4\perp}=2K_{4\perp}/\mu_0 M$, $H_n=2K_n/\mu_0 M$, $H_{4\parallel}=2K_{4\parallel}/\mu_0 M$, and $H_U=2K_U/\mu_0 M$. The shape anisotropy and the second-order anisotropy are both perpendicular to the film; therefore the computer simulation can provide only an overall magnetic anisotropy field:

$$H_{\mathrm{an}} = DM_S - H_n. \quad (2)$$

The time evolution of the magnetization around the equilibrium position was estimated within the Landau-Lifshitz approach, taking into account the damping of the magnetization,[15,16]

$$-\frac{1}{\gamma}\frac{\partial\mathbf{M}}{\partial t} = \mathbf{M}\times\left(-\frac{\partial F}{\partial\mathbf{M}}+\mathbf{h}\right) - \frac{\alpha}{(\gamma M_S)}\left(\mathbf{M}\times\frac{\partial\mathbf{M}}{\partial t}\right), \quad (3)$$

where $\gamma=g\mu_B/\hbar$ and $\alpha=G/\gamma M_s$ are the gyromagnetic ratio and the damping coefficient; g, μ_B, $\hbar$, G, and M_s are the spectroscopic factor, Bohr magneton, Planck constant, Gilbert coefficient, and saturation magnetization; $\mathbf{M}$, F, and $\mathbf{h}(t)$ are the magnetization, the free energy density, and the microwave field, respectively.

The angular dependence of the resonance field at fixed frequency ($f=2\pi\omega$) was computed by considering a drag of the magnetization vector behind the magnetic field. The simulation has reproduced the angular dependence of the resonance field and obtained magnetic anisotropy.[16–19] Without considering the damping effect, the resonance condition is given by

$$\left(\frac{\omega}{\gamma}\right)^2 = \frac{1}{M_S^2\sin^2\theta_0}\left[\frac{\partial^2 F}{\partial\theta^2}\frac{\partial^2 F}{\partial\varphi^2} - \left(\frac{\partial^2 F}{\partial\theta\partial\varphi}\right)^2\right]_{\theta_0,\varphi_0}. \quad (4)$$

The equilibrium angles of the magnetization at resonance (θ_0,φ_0) are imposed by the minimization of the free energy density,[20]

$$\left.\frac{\partial F}{\partial\varphi}\right|_{\theta_0,\varphi_0} = 0 \text{ and } \left.\frac{\partial F}{\partial\theta}\right|_{\vartheta_0,\varphi_0} = 0. \quad (5)$$

Considering Eqs. (1), (4), and (5), the resonance condition for the magnetic field can be derived as

$$\left(\frac{\omega}{\mu_0\gamma}\right)^2 = [(H_0a_1+b_1)(H_0a_1+b_2)-b_3^2]. \quad (6)$$

Here,

$$a_1 = \cos\theta\cos\theta_H + \sin\theta\sin\theta_H\cos(\varphi-\varphi_H),$$

$$b_1 = -\left[H_{\mathrm{an}} + H_U\cos^2\left(\varphi+\frac{\pi}{4}\right)\cos 2\theta + H_{4\perp}\right] \times\frac{\cos 2\theta+\cos 4\theta}{2} + H_{4\parallel}\frac{\cos 4\theta-\cos 2\theta}{2}\frac{3+\cos 4\varphi}{4},$$

$$b_2 = -H_{\mathrm{an}}\cos^2\theta + H_{4\perp}\cos^4\theta + H_{4\parallel} \times\sin^2\theta\left(\cos 4\varphi - \cos^2\theta\frac{3+\cos 4\varphi}{4}\right) - H_U\left\{\sin 2\varphi + \left[\cos\theta\cos\left(\varphi+\frac{\pi}{4}\right)\right]^2\right\},$$

and $b_3 = 0.5\cos\theta(1.5H_{4\parallel}\sin 4\varphi\sin^2\theta + H_U\cos 2\varphi)$.

A nonlinear fitting algorithm has been used for the analysis of the angular dependence of resonance field. This algorithm minimizes the multiparameter χ^2 function and obtains the anisotropy magnetic field parameters (H_U, $H_{4\parallel}$, H_{an}, and $H_{4\perp}$). Since the resonance field depends on the sample

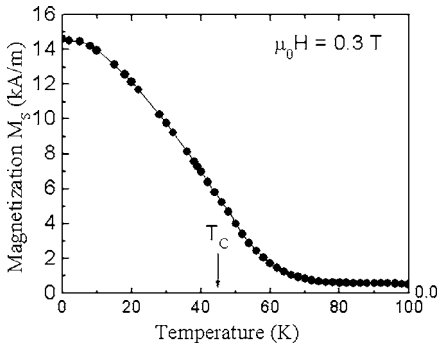

FIG. 2. The temperature dependences of the magnetization at saturation (M_S).

magnetization it was assumed for simplicity that the magnetic field and the magnetization are in the same plane ($\varphi = \varphi_H = 45°$ for configuration *A*, and $\theta = \theta_H = 90°$ for configuration *B*). Moreover the skin depth of the microwave radiation in $Ga_{1-x}Mn_xAs$, $\delta = \sqrt{2/\mu_R\mu_0\omega\sigma} \sim 2$ μm, is much larger than the thickness of the film. This assures that the microwave field is constant everywhere inside the film. Considering a drag of the magnetization induced by the magnetic field, the calculation of the resonance field starts from the condition of free energy density minimum [Eq. (4)]. For each orientation of the applied field, the equilibrium direction of the magnetization (**M**) and the resonance magnetic field ($\mathbf{H}_0$) were calculated [Eqs. (5) and (6)].

IV. EXPERIMENTAL RESULTS

The magnetization of the sample was measured in two external magnetic fields (0.005 and 0.3 T) applied parallel with the surface (e.g., [110] direction), and in increasing temperature (from 5 to 100 K) by using a SQUID magnetometer. The hysteresis measurements performed in magnetic field up to 1 T have indicated that the saturation magnetic field is around 0.3 T and the magnetization at saturation increases with the decrease in temperature. Considering n_{Mn} (the number of Mn atoms per m^3), n_B (the number of Bohr magneton per Mn ion), and S_{Mn} (their spin), the volume magnetization of the sample can be written as $M = n_{\mathrm{Mn}} g \mu_B S_{\mathrm{Mn}} = n_{\mathrm{Mn}} n_0 \mu_B$. The g factor is 2 for the Mn ions and the spin of the Mn^{2+} ions (S_{Mn}) is 5/2. The shape anisotropy at 0 K and 0.3 T was $\mu_0 M_S^2/2 = 134 \pm 7.5$ J/m^3. The temperature dependence of the magnetization is shown in Fig. 2. The number of Bohr magneton per Mn ion and the magnetization at saturation at 0 K were estimated[17] from a long spin wave $T^{3/2}$: $n_B(0) = 2.0 \pm 0.3$ and $M_{\mathrm{sat}}(0) = 14.6 \pm 0.4$ kA/m. The magnetization measurements in 0.005 T have suggested a Curie point about 45 ± 1 K by a sharp transition point. For the simulation of the angular dependence of the ferromagnetic resonance field we have used the SQUID measured magnetization in a magnetic field of 0.3 T.

The angular dependence of FMR spectra was analyzed at various temperature below Curie point T_C in the *X* band ($f = 9.479$ GHz). FMR resonance spectra measured at angles θ_H from 0° to 90° at $T = 30$ K for the out-of-plane configuration *A* are plotted in Fig. 3. The positions of the resonance lines were accurately measured by fitting the FMR signal with the

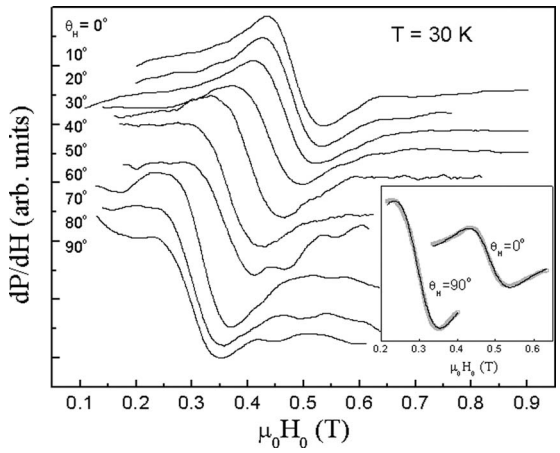

FIG. 3. FMR resonance spectra measured at angles θ_H from 0° to 90° at 30 K. Inset: FMR resonance spectra measured at angles $\theta_H = 90°$ and 180°. The broad gray line represents the best fit of the resonance line, assuming a Lorentzian shape.

first derivative of a symmetric Lorentzian curve (see inset in Fig. 3). The obtained angular dependence of the resonance line position H_0 for configuration *A* at various temperatures is shown in Fig. 4. It is observed that at low temperatures the angular dependence of H_0 shows fourfold symmetry while near the Curie point a twofoldlike symmetry was recorded. This indicates that the relative contribution of the second-order anisotropy ($K_{\mathrm{an}} = \mu_0 M^2/2 - K_n$) becomes larger than the fourth-order anisotropy ($K_{4\parallel}, K_{4\perp}$), as the temperature of the sample is increased towards Curie temperature, in agreement with the theoretical simulation (see Fig. 5). The solid lines in Fig. 4 represent the best fits of experimental data, obtained by using Eqs. (4)–(6) and assuming $g = 2.00$. The experimental data and the simulated curves agree with each other at every temperature. It should be noticed that the fourth-order magnetic anisotropy terms ($K_{4\parallel}, K_{4\perp}$) have to be considered for a correct simulation of the angular dependence of the resonance field. If the term $K_{4\perp}$ is neglected, the simulated curves (see the dashed lines in Fig. 4) do not match the measured resonance fields for the normal orientation of the

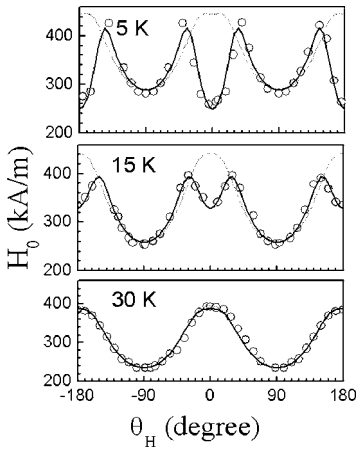

FIG. 4. The angular dependence of the resonance field at 5, 15, and 30 K. Experimental data points (open circle) and simulated lines (solid and dashed lines) are plotted. Note that the solid line represents the simulation with $H_{4\perp}$ term, while the dash line represents the simulation without $H_{4\perp}$ term.

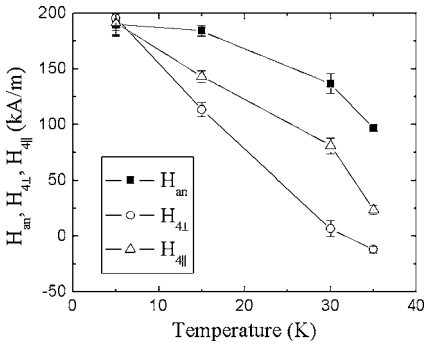

FIG. 5. The temperature dependence of the second-order (H_{an}) and fourth-order ($H_{4\parallel}$ and $H_{4\perp}$) magnetic anisotropies.

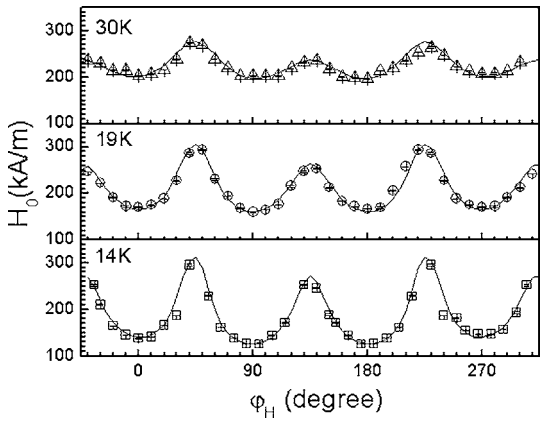

FIG. 6. The in-plane angular dependence of the resonance magnetic field at various temperatures. The lines represent the best fit of experimental data.

external field and for temperatures lower than 30 K. The temperature dependence of magnetocrystalline anisotropies of second and fourth orders obtained in the computer simulation of the angular dependence of FMR positions for the out-of-plane configuration *A* is shown in Fig. 5. The absolute values of the second- and fourth-order magnetic anisotropies decrease as the temperature of the sample is increased.

To verify the existence of the in-plane cubic anisotropy $K_{4\parallel}$, FMR measurements in the in-plane configuration *B* (magnetic field rotated in the plane of the sample) were carried out at 14, 19, and 30 K. The experimental results are shown in Fig. 6. It is observed that the resonance field position presents a fourfold in-plane symmetry (distorted by a small twofold anisotropy) at all temperatures. Maximum resonance fields recorded for $\varphi_H=45°$, 135°, 225°, and 315° and minima located at 0°, 90°, 180°, and 270° indicate that the in-plane easy (and hard) magnetization axis is along the ⟨100⟩ (and ⟨110⟩) crystallographic directions, respectively. The lines in Fig. 6 represent the best fit of experimental data obtained by using Eq. (6). An excellent correlation between theoretical predictions and experimental data was obtained. Finally, the obtained magnetic anisotropy shows that the uniaxial in-plane magnetic anisotropy (H_U) has weak temperature dependence in the limit of the experimental errors. However, the other magnetic anisotropy parameters ($H_{4\parallel}$ and H_{an}) decrease with the increase in temperature.

V. DISCUSSIONS AND CONCLUSIONS

The effective *g* factor for $Ga_{1-x}Mn_xAs$ was reported elsewhere.[21] There are a group of lines at $g=2.00$ identified as the $\Delta M=1$ transition of the ionized Mn ($3d^5$) acceptor A^-, and another two groups of lines at $g=2.77$ and $g=5.72$ corresponding to the $\Delta M=2$ and $\Delta M=1$ transitions of the spin 1 state. Since the recorded resonance lines had an evident angular dependence they originated from the well known ionized Mn ($3d^5$) acceptor A^-.[22,23] The resonance lines observed in this paper show a strong angular dependence, and converge to a resonance determined by $g=2.00$ as we approach the Curie temperature. We have therefore used $g=2.00$ as the *g* factor corresponding to the state of the Mn ion in the GaAs host

The effective magnetic anisotropy ($K_{an}=\mu_0 M^2/2-K_n$) is positive, suggesting an in-plane easy magnetization direction ($\theta_{eq}=90°$). The direction of the in-plane magnetization axis is given by the sign of the in-plane fourth-order magnetic anisotropy. The calculated positive value for $K_{4\parallel}$ suggests that the in-plane easy axis is parallel with the ⟨100⟩ crystalline directions for the $Ga_{1-x}Mn_xAs$ sample with $x=3.5\%$ Mn concentration. This result was absolutely confirmed by the measurement carried out in the in-plane configuration *B*. Moreover, a fourth-order magnetic anisotropy perpendicular to the substrate ($K_{4\perp}$) has to be considered for simulation of the angular dependence of FMR positions for the out-of-plane configuration *A*, especially for low temperature. The existence of $K_{4\perp}$ in $Ga_{1-x}Mn_xAs$ sample with low Mn concentration indicates the cubic symmetry of $Ga_{1-x}Mn_xAs$ system in the growth direction (i.e., *z* direction) has not been destroyed by the tetragonal distortion from the strain induced by the lattice mismatch between the $Ga_{1-x}Mn_xAs$ film and the GaAs substrate.

ACKNOWLEDGMENTS

We thank Robert Addleman for his technical support during our measurements performed in the Chemistry Department at Indiana University-Bloomington. This study was supported by the 21st Century Science and Technology Fund of Indiana and by the DARPA/SpinS Programs through the Office of Naval Research.

[1] S. D. Bader, Proc. IEEE **78**, 909 (1990).
[2] S. A. Haque, A. Matsuo, Y. Yamamoto, and H. Hori, J. Magn. Magn. Mater. **247**, 117 (2002).
[3] J. Meckenstock, D. Spoddig, K. Himmelbauer, H. Kren, M. Doi, W. Keune, Z. Frait, and J. Pelz, J. Magn. Magn. Mater. **240**, 410 (2002).
[4] H. Ohno, Science **281**, 951 (1998).
[5] Y. Sasaki, X. Liu, J. K. Furdyna, M. Palczewska, J. Szczytko, and A. Twardowski, J. Appl. Phys. **91**, 7484 (2002).
[6] T. Hartmann, M. Lampalzer, P. J. Klar, W. Stolz, W. Heimbrodt, H.-A. Krug von Nidda, A. Loidl, and L. Svistov, Physica E (Amsterdam) **13**, 572 (2002).
[7] K. Dziatkowski, M. Palczewska, T. Slupinski, and A. Twardowski, Phys. Rev. B **70**, 115202 (2004).
[8] X. Liu, Y. Sasaki, and J. K. Furdyna, Phys. Rev. B **67**, 205204 (2003).
[9] M. Farle, Rep. Prog. Phys. **61**, 755 (1998).
[10] H. Ohno, A. Shen, F. Matsukura, A. Oiwa, A. Endo, S. Katsumoto, and Y. Iye, Appl. Phys. Lett. **69**, 363 (1996).
[11] J. K. Furdyna, X. Liu, and Y. Sasaki, J. Appl. Phys. **91**, 7490 (2002).
[12] J. Konig, J. Schliemann, T. Jungwirth, and A. H. MacDonald, in *Electronic Structure and Magnetism of Complex Materials*, edited by D. J. Singh and D. A. Papaconstantopoulos (Springer, Berlin, 2002).

[13]M. Farle, B. Mirwald-Schulz, A. N. Anisimov, W. Platow, and K. Baberschke, Phys. Rev. B **55**, 3708 (1997).
[14]R. F. Pearson, in *Experimental Magnetism* edited by G. M. Kalvius and R. S. Tebble (Wiley, New York, 1979), Vol. 1, p. 138.
[15]A. Aspelmeier, M. Tischer, M. Farle, M. Russo, K. Baberschke, and D. Arvamitis, J. Magn. Magn. Mater. **146**, 256 (1995).
[16]J. F. Cochran, J. M. Rudd, M. From, B. Heinrich, W. Bennett, W. Schwarzacher, and W. F. Egelhoff, Phys. Rev. B **45**, 4676 (1992).
[17]S. V. Vonsovskii, *Ferromagnetic Resonance* (Pergamon, Oxford, 1966), p. 67.
[18]F. Gerhardter, Y. Li, and K. Baberschke, Phys. Rev. B **47**, 11204 (1993).
[19]R. Mechenstock, D. Spoddig, K. Himmelbauer, H. Krenn, M. Doi, W. Keune, Z. Frait, and J. Pelzl, J. Magn. Magn. Mater. **240**, 410–413 (2002).
[20]A. Z. Maksymowicz and K. D. Leaver, J. Phys. F: Met. Phys. **3**, 1031 (1973).
[21]J. Schneider, U. Kaufmann, W. Wilkening, M. Baeumler, and F. Kohl, Phys. Rev. Lett. **59**, 240 (1987).
[22]N. Almeleh and B. Goldstain, Phys. Rev. **128**, 1568 (1962).
[23]R. Bleekrode, J. Dielman, and H. J. Vegter, Phys. Lett. **2**, 355 (1962).